Identification of Redox Sensitive Thiols of Protein Disulfide Isomerase Using Isotope Coded Affinity Technology and Mass Spectrometry

Anna Kozarova, Inga Sliskovic and Bulent Mutus
Department of Chemistry and Biochemistry, University of Windsor, Windsor, Ontario, Canada

Eric S. Simon and Philip C. Andrews
Department of Biological Chemistry, University of Michigan, Ann Arbor, Michigan, USA

Panayiotis O. Vacratsis
Department of Chemistry and Biochemistry, University of Windsor, Windsor, Ontario, Canada

Regulation of the redox state of protein disulfide isomerase (PDI) is critical for its various catalytic functions. Here we describe a procedure utilizing isotope-coded affinity tag (ICAT) technology and mass spectrometry that quantitates relative changes in the dynamic thiol and disulfide states of human PDI. Human PDI contains six cysteine residues, four present in two active sites within the *a* and *a′* domains, and two present in the *b′* domain. ICAT labeling of human PDI indicates a difference between the redox state of the two active sites. Furthermore, under auto-oxidation conditions an ~80% decrease in available thiols within the *a* domain was detected. Surprisingly, the redox state of one of the two cysteines, Cys-295, within the *b′* domain was altered between the fully reduced and the auto-oxidized state of PDI while the other *b′* domain cysteine remained fully reduced. An interesting mono- and dioxidation modification of an invariable tryptophan residue, Trp-35, within the active site was also mapped by tandem mass spectrometry. Our findings indicate that ICAT methodology in conjunction with mass spectrometry represents a powerful tool to monitor changes in the redox state of individual cysteine residues within PDI under various conditions. (J Am Soc Mass Spectrom 2007, 18, 260–269) © 2007 American Society for Mass Spectrometry

Protein disulfide isomerase (PDI), a member of the thioredoxin superfamily of redox proteins, is an enzyme responsible for disulfide bond formation and isomerization [1, 2], redox-dependent chaperone function [3, 4] and S-nitrothiols denitrosation activity [5]. Originally, PDI was identified in the lumen of the endoplasmatic reticulum [6, 7] and subsequently detected at additional locations, such as the cell surface and the cytosol [8]. In the case of secreted PDI, it has been demonstrated to control the redox state of certain cell-surface proteins [9]. Furthermore, PDI was identified as a subunit of prolyl 4-hydroxylase [10, 11] and microsomal triglyceride transfer protein [12, 13], executing different functions than in its monomeric state.

PDI comprises four domains, *a*, *b*, *b′*, and *a′* [14] and an acidic region designated *c* [15–17] (Figure 1a). The two thioredoxin domains of PDI [18], *a* and *a′*, each contain an active site with a consensus sequence *W***C**GH**C**K, which are separated by two thioredoxin-like domains *b* and *b′*. The multi-domain structure of PDI is required to catalyze thiol-disulfide exchange events and effect folding by inducing conformational changes in the substrate protein [19]. Recently, the crystal structure of yeast PDI was elucidated and the structure revealed thioredoxin domains arranged in a shape of a twisted "U" with the active sites facing each other across the "U" [20].

Each PDI molecule contains six cysteine residues. Four of them have been shown to participate in the redox activity and are present as two vicinal thiol groups within each active site. Multiple studies have investigated the relative redox/catalytic contributions of the two thioredoxin active sites, and have suggested that they do not have equivalent catalytic properties [16, 21]. Furthermore, the NMR structure of human PDI *a* domain identified Cys-36, as accessible and exposed while Cys-39, as buried and con-

Published online October 30, 2006

Address reprint requests to Dr. P. O. Vacratsis, Department of Chemistry and Biochemistry, University of Windsor, 401 Sunset Avenue, Windsor, ON N9B 3P4, Canada. E-mail: vacratsi@uwindsor.ca

1044-0305/07/$32.00
doi:10.1016/j.jasms.2006.09.023

Received June 21, 2006
Revised August 29, 2006
Accepted September 27, 2006

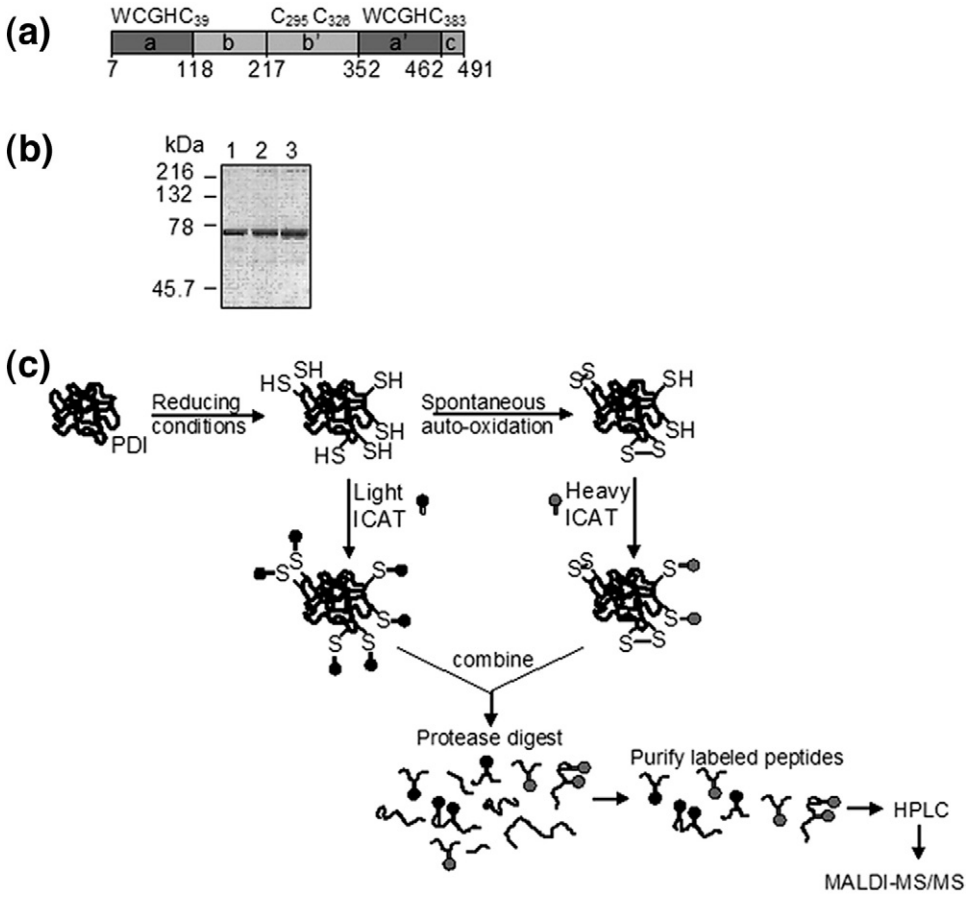

Figure 1. Schematics of ICAT strategy. (**a**) A schematic model of domain architecture of human PDI. Domains *a*, *b*, *b*′, and *a*′ share a common thioredoxin fold, but only the *a* and *a*′ domain have the *WCXX***C** active site. Position of all six cysteine residues within human PDI is highlighted. (**b**) Bacterially expressed, purified human His-PDI was separated using SDS-PAGE (10%) and visualized by Coomassie blue stain. Lane 1, PDI control purchased from Sigma; lane 2, reduced His-PDI (treated with 5x excess DTT); lane 3, auto-oxidized His-PDI (following reduction, PDI was incubated in phosphate buffer for 1 h at room-temperature). (**c**) Schematic presentation of ICAT labeling protocol. PDI was reduced and immediately labeled with light ^{12}C-ICAT reagent or incubated at room temperature to allow auto-oxidation and subsequently labeled with heavy ^{13}C-ICAT reagent and processed as described in the Materials and Methods section.

strained [22]. In addition, the crystal structure of yeast PDI is consistent with the view that the two cysteines within the *a* domain are primarily in the oxidized state (modeled as a mixture of oxidized to reduced state at 0.8 to 0.2, respectively) and the cysteines within the *a*′ domain are in a reduced state [20]. The function and regulation of the redox states of the other two cysteine residues present within the *b*′ domain of human PDI, remains unclear.

The redox state of the active site cysteines dictates the type of reaction PDI will catalyze. Introducing disulfide bonds into a protein substrate requires the presence of a disulfide active site, while rearranging disulfide bonds within a protein substrate requires the presence of a dithiol active site [1, 21, 23]. Therefore, the dithiol/disulfide balance within the active sites is required for effective oxidation or disulfide formation on PDI substrates [23]. Furthermore, alterations of this redox state balance of PDI underlie different pathological conditions. For example, it has been observed that upon activation/aggregation of resting platelets, the amount of reduced dithiols on cell surface PDI increased approximately 3-fold, thus implying that thiol groups are critical for platelet aggregation [24].

Common approaches to analyze thiol oxidation states include spectrophotometric and fluorescence-based assays [25], however, these only provide information regarding the average number of modified cysteine residues, not their exact identity. Here, we present a method that uses isotope-coded affinity tag (ICAT) based method in conjunction with mass spectrometry (MS) [26, 27] to detect and quantitate relative dynamic changes in the thiol oxidation state of individual cysteine residues in recombinant human PDI under reducing and auto-oxidizing conditions.

In addition to the detection of the redox status of the active site cysteines, we will offer data indicating redox regulation of Cys-295 present within the *b′* domain. Also, a novel oxidation modification on an invariable tryptophan residue, Trp-35, adjacent to the cysteine residues within the active site, will be presented.

Materials and Methods

Purification of Protein Disulfide Isomerase

His-PDI was expressed and purified as described previously [5]. Protein quantification was performed using the Bradford assay [28] and protein purity was ascertained by SDS-PAGE.

PDI Reduction and Spontaneous Auto-Oxidation

Bacterially expressed human His-PDI (100 μg) was fully reduced with 5× molar excess of DTT for 2 h at room temperature. The DTT was removed during gel-filtration on Sephadex G-25 in 100 mM phosphate buffer, pH 7. Immediately after separation, the reduced PDI was acetone precipitated and labeled with light ^{12}C-ICAT reagent (Applied Biosystems, Foster City, CA). For spontaneous auto-oxidation, PDI was incubated for 1 h at room temperature following the reduction with DTT and gel-filtration. Subsequently, this sample was also acetone precipitated and labeled with heavy ^{13}C-ICAT reagent (Applied Biosystems).

ICAT Labeling of Reduced and Auto-Oxidized PDI

PDI containing samples were prepared as described above and ICAT labeling and purification of labeled peptides was performed following the provided protocol from Applied Biosystems. Experiments were performed three times to ensure reproducibility of the results. Briefly, reduced and auto-oxidized PDI was labeled with ^{12}C-ICAT and ^{13}C-ICAT reagents, respectively, for 2 h at 37 °C. After alkylation with the iodoacetamide-based ICAT reagent, the two samples were mixed together and subjected to digestion with Endoproteinase *Glu-C* for 12 h at 25 °C. Peptides were desalted using a cation exchange cartridge provided in the Applied Biosystems kit, and biotin labeled peptides were purified using an avidin affinity cartridge present in the kit. Peptides were subsequently dried and resuspended in the cleavage reagent to release the labeled peptides from the biotin moiety by incubation for 2 h at 37 °C. Subsequently, peptides were dried and resuspended in 1% formic acid. All samples were desalted using micro-C_{18} ZipTips (Millipore, Billerica, MA) before MALDI MS analysis.

HPLC Separation of ICAT Labeled Peptides

ICAT labeled peptides were separated on a LC Packings nanoflow HPLC system (nano-LC) (LC Packings, Sunnyvale, CA) with a Zorbax 300 SB C_{18} column (75 μm × 150 mm, 3.5 μm particles) (Agilent Technologies, Palo Alto, CA) at a flow rate of 300 nL/min. These peptides were separated using multi-step linear gradient of 0 to 30% B in the first 10 min, followed by 30 to 45% B for 37 min, 45 to 60% B for 5 min and 100% B for 6 min (mobile phase A, 3% acetonitrile, 0.1% trifluoroacetic acid; mobile phase B, 90% acetonitrile, 0.1% trifluoroacetic acid). Column effluent was mixed with MALDI matrix (2 mg/ml α-cyano-4-hydroxycinnamic acid, 10 mM ammonium dihydrogen phosphate in 50:49:1 water/isopropyl alcohol/acetic acid) through a mixing tee and spotted automatically with a Probot (LC Packings) onto a 192-well MALDI target plate. The matrix was delivered to the mixing tee at a flow rate of 1.2 μL/min.

Mass Spectrometry Analysis

ICAT labeled peptides were analyzed by MALDI-TOF MS (DE-Pro Voyager, Applied Biosystems) and MALDI-TOF/TOF (4700 Proteomics Analyzer, Applied Biosystems/MDX Sciex). For the MALDI-TOF MS analysis, the purified labeled peptide sample (1:1 matrix solution α-cyano-4-hydroxycinnamic acid) was spotted onto a MALDI target plate and analyzed in reflector mode. For the MALDI-TOF/TOF analysis MS and MS/MS spectra were acquired in positive ion reflector mode. MS survey scans were acquired first for each MALDI well and the ions of interest were selected, with the time ion gate set at 3 Da (±), for MS/MS analysis.

Results and Discussion

ICAT Labeling of PDI

An ICAT-labeling approach in combination with mass spectrometry was developed for the purpose of quantitating changes in the redox state of human His-PDI under various conditions, since only free thiols will react with the iodoacetamide-based ICAT reagent. Bacterially expressed human PDI was purified to near homogeneity by nickel chromatography (Figure 1b). To assess if PDI can be labeled with ICAT reagent, following reduction with excess reducing agent, the free thiol groups on cysteine residues (cysteine-SH) were initially incubated with acid-cleavable light ^{12}C-ICAT reagent only. The ICAT-labeled protein was digested with *Glu-C* to generate unique peptides corresponding to each active site. The [MH^+] 2147 *m/z* ion represents the peptide containing the active site within the *a* domain, FYAPWC_{36}GHC$_{39}$KALAPE, containing two ICAT labels (molecular mass 227 Da per one ICAT-tag) (Figure 2a). This indicates that both cysteines within

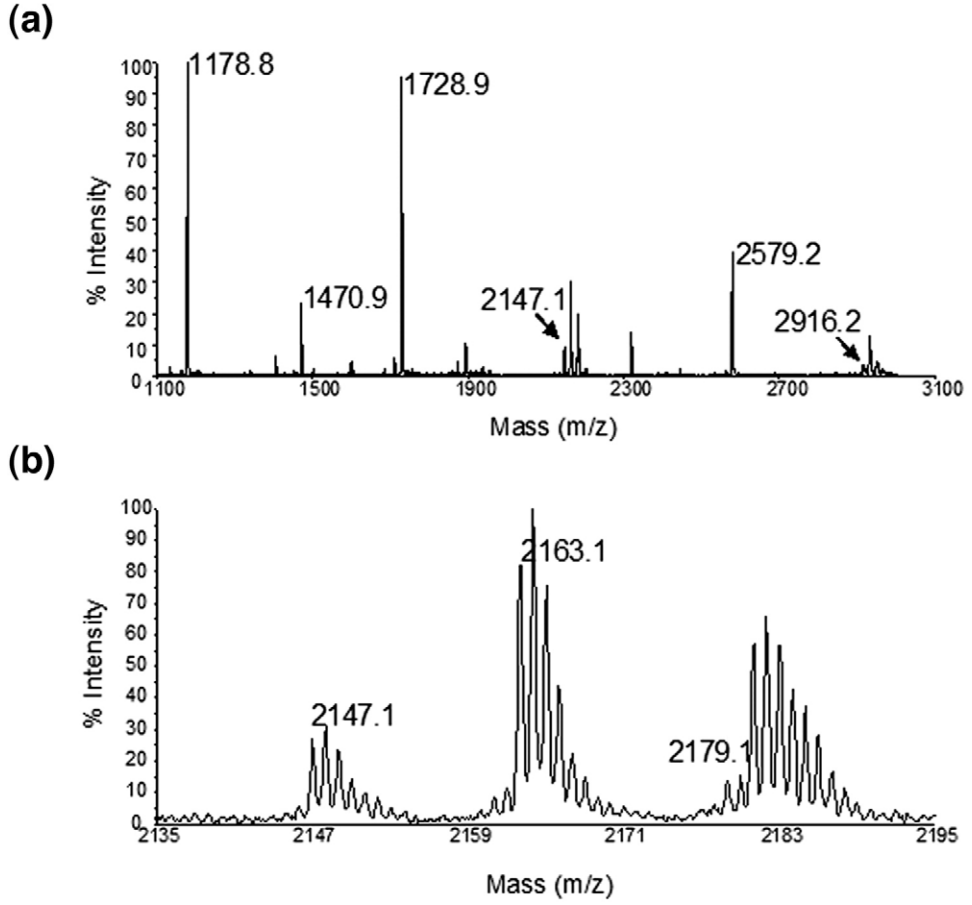

Figure 2. Reduced PDI labeled with light ^{12}C-ICAT reagent. (**a**) Full scan MALDI-TOF spectrum of ICAT-labeled *Glu-C* digested peptides from PDI. The [MH$^+$] 2147 *m/z* fragment corresponds to the *a* domain active site with both Cys residues ICAT labeled. The [MH$^+$] 2916 *m/z* fragment corresponds to the *a′* domain active site with both Cys residues ICAT labeled. The additional peptide fragments are presented in tabulated form, including the theoretical mass prior to Cys modification and after modification with corresponding detected ions, i.e., the fragment at [MH$^+$] 1178 *m/z* corresponds to the Cys-326 present in the *b′* domain while fragments at [MH$^+$] 1470 *m/z*, [MH$^+$] 1728 *m/z*, and [MH$^+$] 2579 *m/z* represent various miscleavages of the sequence containing Cys-295. (**b**) Enlargement from (**a**) (range 2135 to 2195 *m/z*) showing the ions corresponding to addition of +16 Da and +32 Da on the *a* domain active site peptide.

the *a* domain were in the reduced state and thus susceptible to labeling with the ICAT alkylating agent (confirmed by analysis of MS/MS fragment ion series, as described below). Importantly, we did not detect a peak at [MH$^+$] 1924 *m/z*, which would correspond to only one ICAT-labeled cysteine residue. Similarly to the *a* domain active site, a peptide fragment representative of the *a′* domain active site at [MH$^+$] 2916 *m/z* was modified with two ICAT labels. However, further analysis was complicated with the inability of reproducibly detecting this peptide. This implies that under these conditions, cysteine residues within the *a′* domain peptide FYAPWC$_{380}$GHC$_{383}$KQLAPIWDKLGE, are either buried and inaccessible to the ICAT moiety or exist predominantly in their oxidized form, in agreement with

Table 1. Recombinant human PDI ICAT-labeled peptides.

No.	Start	End	Cys	Sequence	Mass (monoisotopic) (m/z)	^{12}C-ICAT-modified (m/z) calculated	^{12}C-ICAT-modified (m/z) observed
1	325	331	326	FCHRFLE	951.5	1178.6	1178.8
2	294	304	295	ECPAVRLITLE	1243.6	1470.7	1470.9
3	294	306	295	ECPAVRLITLEEE	1501.8	1728.9	1729.0
4	31	45	36,39	FYAPWCGHCKALAPE	1692.7	2147.0	2147.1
5	287	306	295	FFGLKKEECPAVRLITLEEE	2351.2	2578.3	2579.3
6	375	395	380,383	FYAPWCGHCKQLAPIWDKLGE	2462.2	2916.4	2916.2

other studies [5, 21], and are therefore less susceptible to ICAT modifications.

In addition, peptide fragments corresponding to the two remaining cysteine residues of the PDI within the *b′* domain were also detected (Figure 2a, and Table 1). Numerous peptides were detected encompassing the ICAT-labeled cysteine at position 295, specifically EC_{295}PAVRLITLE ([MH^+] 1470 *m/z*) and two peptides corresponding to additional miscleavages ([MH^+] 1729 *m/z* and [MH^+] 2579 *m/z*). The [MH^+] ion detected at 1178 *m/z* corresponded to the other cysteine within the *b′* domain, Cys-326, within the FC_{326}HRFLE peptide.

Mass spectrometric studies to analyze PDI have been performed in the past. An alternative to the ICAT-based labeling method is alkylation of the cysteine residues with N-ethylmaleimide (NEM) [29]. In parallel to the ICAT labeling described herein, we also modified PDI exposed to reducing conditions with NEM. Fragments corresponding to active sites modified with one or two NEM adducts (125 Da per NEM label) were detected (data not shown). In contrast, the ICAT-modified active site peptides reproducibly produced only peptides labeled on both cysteine residues. Another cysteine alkylating reagent, the episulfonium ion derived from S-(2-chloroethyl)glutathione (CEG) has been identified to modify only one cysteine residue within each active site of rat PDI, Cys-36 and Cys-380 [30]. In addition, cysteine residues of PDI were indicated to be modified by the thiol reactive lipid aldehyde 4-hydroxynonenal (4-HNE) in rat livers fed a combination of high-fat and ethanol diet [31], although the modified cysteines were not resolved. Overall, these different thiol reactivities may be due to incomplete labeling caused by various degrees of hydrophobicity and hydrophilicity of the modifying reagent, resulting in limited access to buried and solvent inaccessible regions within PDI. We did not detect any singly labeled vicinal thiols in the active site, indicating the structural nature of the ICAT reagent is capable of reacting with all of the cysteine residues of PDI when they are present in their free thiol form.

Further analysis of the peptide corresponding to the *a* domain active site indicated two sequential peaks (each 16 Da apart) adjacent to the monoisotopic mass of [MH^+] 2147 *m/z* (Figure 2b). These modified light-ICAT labeled peptides would likely complicate the analysis when light and heavy ICAT-modified samples were to be compared. Specifically, the ^{12}C-(light, addition of 227 Da per one ICAT-tag) and ^{13}C-(heavy, addition of 236 Da per one ICAT-tag) reagents have been designed to differ by 9 Da per labeled cysteine residue for quantitation purposes [27]. This would result in an addition of 18 Da when two ICAT labeled cysteines are present within the active site in the *a* domain. Therefore, due to isotopic interference, the discrimination between the +16 Da (light ICAT-label and modified peptide ([MH^+] 2163 *m/z*)) and the + 18 Da (heavy ICAT-label and unmodified peptide ([MH^+] 2165 *m/z*)) peptides would be challenging.

To resolve this issue, ICAT-labeled peptides were fractionated using reverse-phase chromatography (Figure 3). The column elution profile indicated that all of the modified peptides were significantly resolved from each other (Figure 3a), and in expected order. The peptide corresponding to the active site within the *a* domain labeled with two light ICAT-tags and modified by +32 Da eluted first (Figure 3b), followed by the peptide modified by +16 Da (Figure 3c), whereas the most hydrophobic, nonmodified peptide eluted last (Figure 3c).

Tryptophan Oxidation Adjacent to the Active Site Cysteine

MS/MS analysis identified the peptide at [MH^+] 2147 *m/z* to correspond to the *a* domain active site fragment, FYAPWC_{36}GHC_{39}KALAPE. This peptide contains two ICAT labels, one per cysteine residue, as determined from the y_6-y_{10} series, the y_{12} fragment, and the $b_{8'}b_{10}$-b_{14} series (Figure 4a). Further analysis of the fragment ion series indicated that the modified residue on the peptide at 2163 *m/z* and the peptide at 2179 *m/z* was Trp-35. Specifically, the addition of +16 Da ([MH^+] 2163 *m/z*) was consistent with tryptophan mono-oxidation (hydroxytryptophan) (Figure 4b) and the addition of +32 Da ([MH^+] 2179 *m/z*) was due to the tryptophan dioxidized form (*N*-formylkynurenine) (Figure 4c).

This is an intriguing modification since Trp-35 is located within the *a* domain active site immediately adjacent to the active site cysteines. It is possible, that this modification was the result of MS sample preparation. However, it has been argued that tryptophan oxidation is not a considered mass spectrometry encountered artifact, like methionine oxidation [32, 33] and guanidination [34]. Additionally, doubly oxidized tryptophan was identified in a subset of mitochondrial proteins predominantly associated with redox metabolism [33] and in the chaperone α-crystallin from bovine lens tissue exposed to Fenton chemistry [35]. Sequence analysis of the residue surrounding Trp-35 within PDI suggests similarity with these other proteins modified in vivo by tryptophan oxidation.

The susceptibility of the active site tryptophan to oxidation was an unexpected result. In addition, the location of this tryptophan residue immediately adjacent to the active site cysteines suggests that tryptophan oxidation could potentially play a role in regulating PDI catalysis. We are currently pursuing potential oxidation sources and the structural/catalytic consequences of this modification.

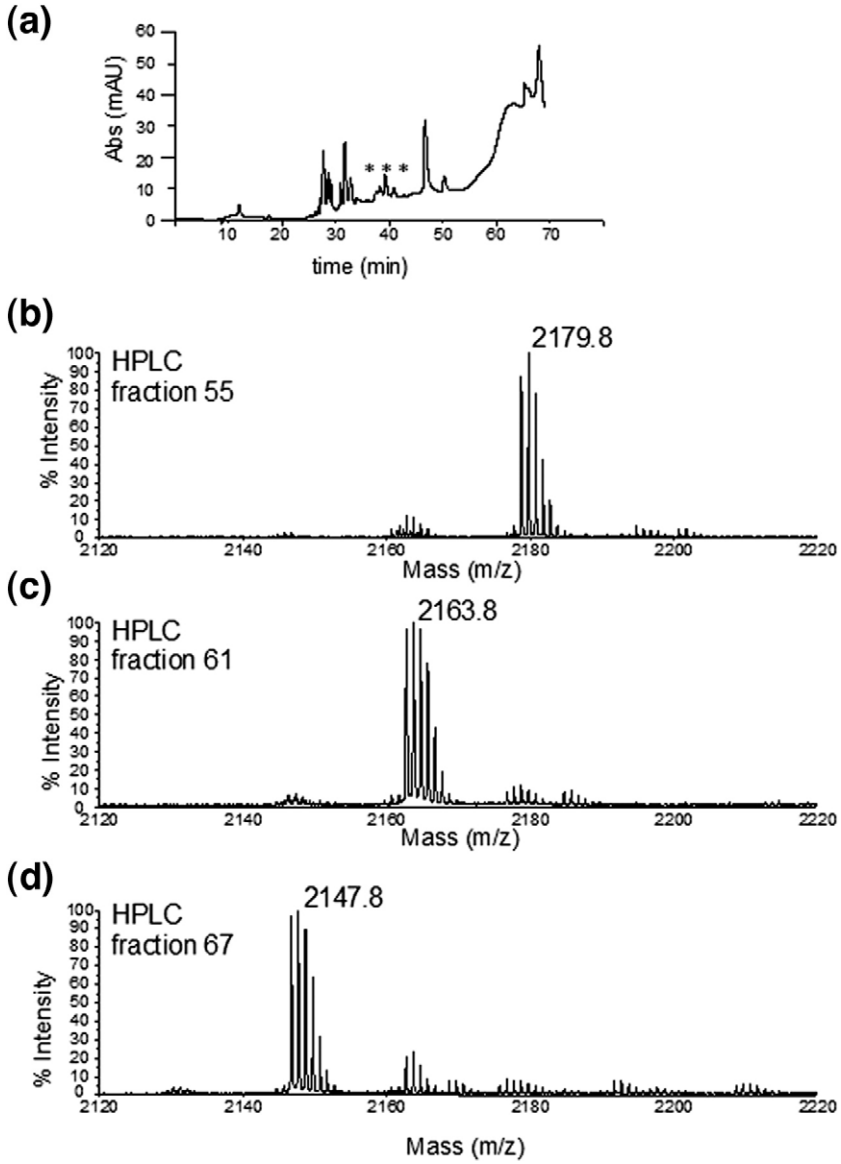

Figure 3. Separation of the modified ^{12}C-ICAT-labeled peptides. (**a**) Chromatogram showing separation of the *Glu-C* digested, ICAT labeled peptides on a reverse-phase nano-LC column. Asterisks indicate elution positions for HPLC fractions 55, 61, and 67 respectively. (**b**) MALDI-TOF analysis of peptides separated by nano-LC. The doubly modified peptide (+32 Da) eluted first ([MH$^+$] 2197 *m/z*), followed by singly modified peptide (+16 Da) ([MH$^+$] 2163 *m/z*) (**c**), and the unmodified peptide ([MH$^+$] 2147 *m/z*) (**d**).

Dynamic Changes in the Redox State of PDI Active Site

We have previously shown that PDI undergoes auto-oxidation in the absence of reducing agents [5]. To further characterize and definitively identify the cysteine residues altered during auto-oxidation, the ICAT strategy was used to quantify changes in the redox state of PDI. Specifically, reduced PDI was labeled with the light ^{12}C-ICAT reagent, while auto-oxidized PDI was labeled with the heavy ^{13}C-ICAT reagent (Figure 1c). These samples were subsequently combined and processed together. Upon fractionation of PDI peptides by nano-LC, the relative quantity of thiol oxidation was assessed by MS. For the purified *a* domain peptides, there was a significant loss of ICAT labeling under these auto-oxidized conditions. Although coeluting peptides complicated precise quantitation, all tryptophan modified forms displayed approximately a 5 to 1 ratio between reduced and auto-oxidized samples when the most abundant isotope in the two samples were analyzed (Figure 5). The ratio of nonmodified tryptophan containing peptides labeled with ICAT-light reagent (([MH$^+$] 2147 *m/z*) can be compared to nonmodified tryptophan containing peptides labeled with ICAT-

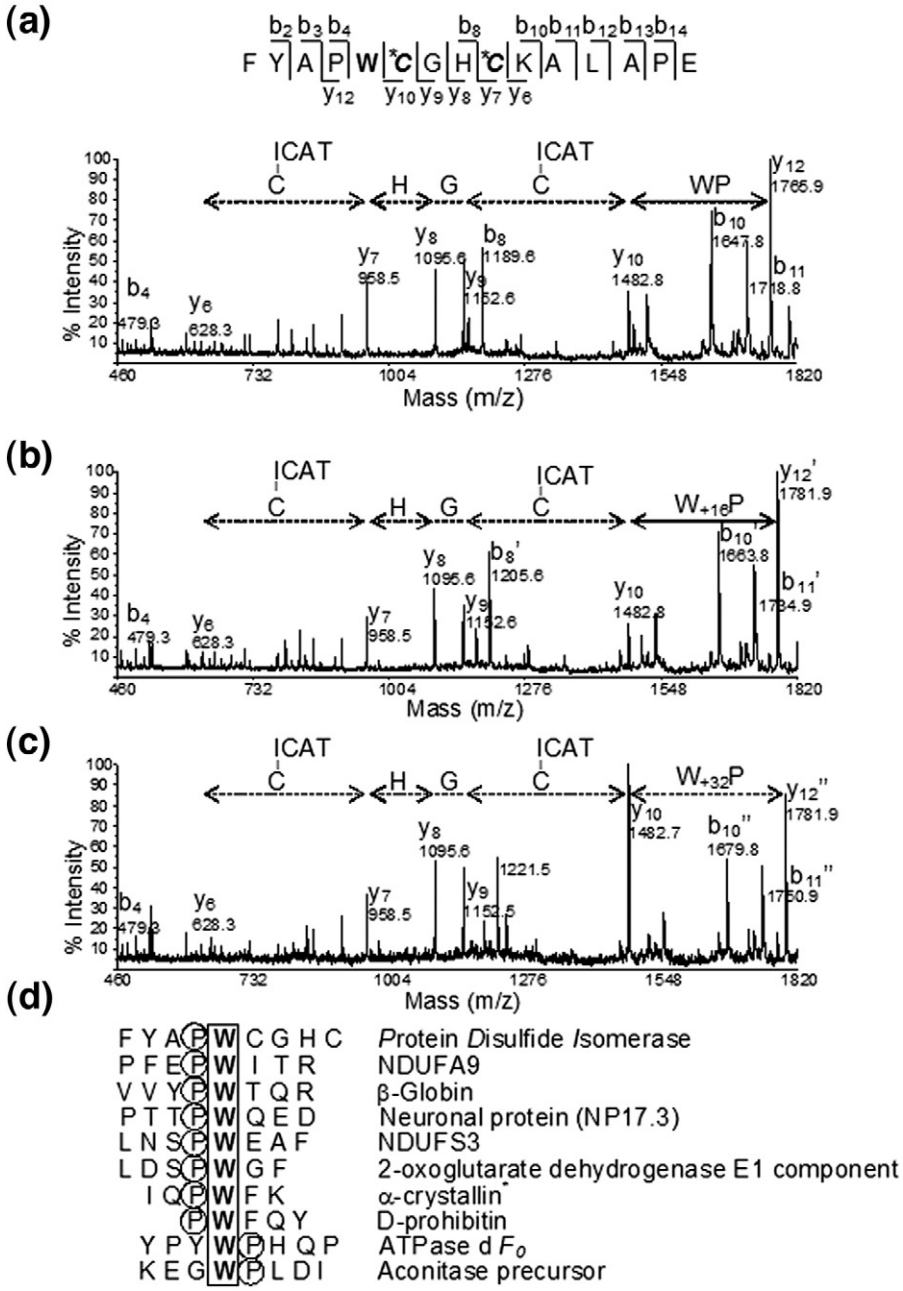

Figure 4. MALDI-TOF MS/MS analysis of the *a* domain active site labeled with light ^{12}C-ICAT reagent displaying tryptophan oxidation. (**a**) MS/MS spectrum of the unmodified peptide ([MH$^+$] 2147 *m/z*) showing the amino acid sequence and position of ICAT modifications. (**b**) The +16 Da modified peptide ([MH$^+$] 2163 *m/z*) was determined to contain a hydroxytryptophan. (**c**) The +32 Da modified peptide ([MH$^+$] 2179 *m/z*) was determined to contain a doubly oxidized tryptophan, N-formylkynurenine. Asterisks within the sequence indicates modification of cysteine residues with ICAT reagent, (prime) indicates modification of the y- and b-ions by +16 Da (**b**), and (double prime) indicates modification by + 32 Da (**c**). (**d**) Sequence alignment of peptides identified to contain doubly oxidized tryptophan; these peptides were identified in the cardiac mitochondrial proteome [33] and from bovine intact lens (asterisk) [35].

heavy reagent ([MH$^+$] 2165 *m/z*) (Figure 5c). The ratio of the light and heavy ICAT labeled hydroxytryptophan containing peptides ([MH$^+$] 2163 *m/z* and [MH$^+$] 2181 *m/z*) was consistent to the tryptophan unmodified peptides (Figure 5b) as was the case of the N-formylkynurenine containing peptides ([MH$^+$] 2179 *m/z* and [MH$^+$] 2197 *m/z*) (Figure 5a). Finally, the consistent ratio between the tryptophan modified peptides indicates that the tryptophan oxidation does not affect the redox state of the active site cysteine residues.

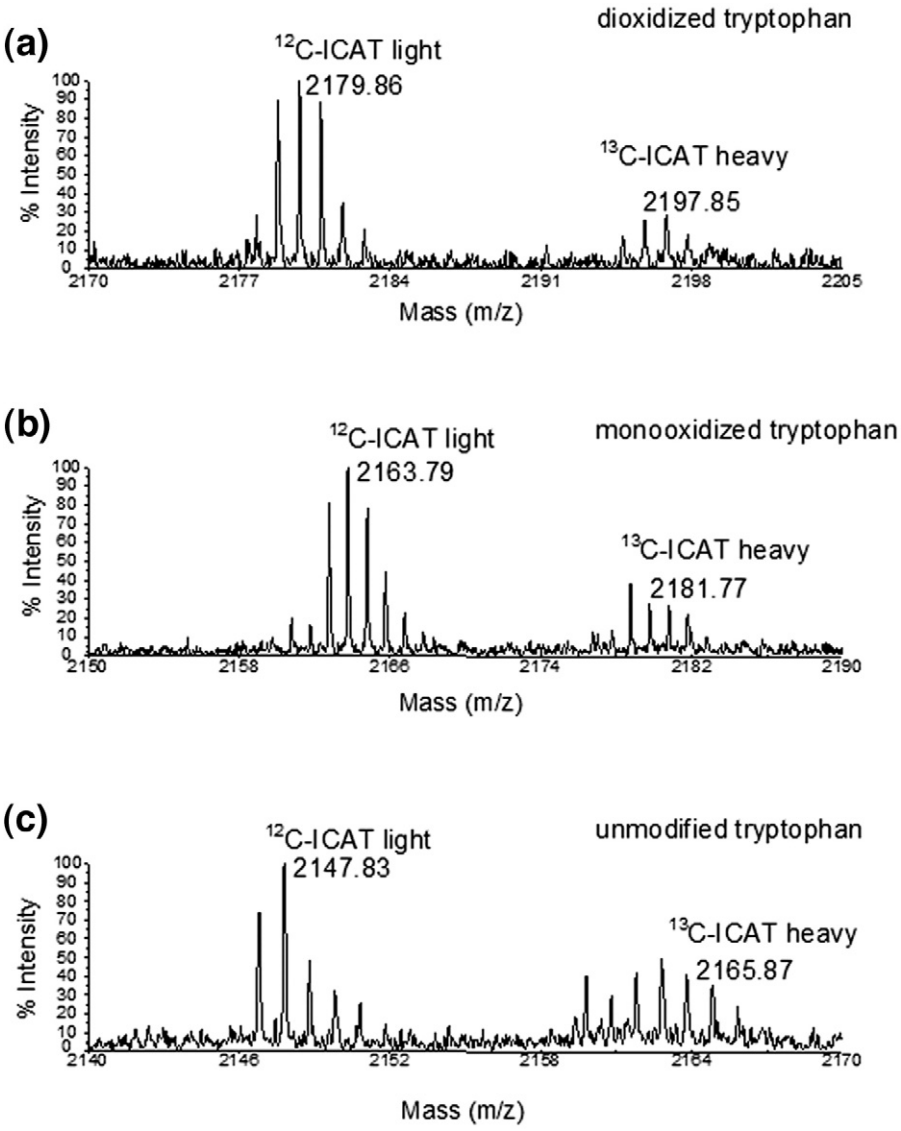

Figure 5. Quantitation of reduced (light ^{12}C-ICAT-labeled) and auto-oxidized (heavy ^{13}C-ICAT-labeled) PDI following reverse-phase nano-LC separation. (**a**) Peptides corresponding to the *a* domain active site containing the doubly oxidized Trp, were detected for reduced PDI (light ICAT labeled, [MH$^+$] 2179 *m/z*) and auto-oxidized PDI (heavy ICAT labeled, [MH$^+$] 2197 *m/z*) displaying ~5-fold decrease in susceptibility to labeling. Peptides corresponding to the *a* domain active site containing the mono-oxidized Trp ([MH$^+$] 2163 *m/z* and 2181 *m/z*) (**b**) and nonmodified Trp ([MH$^+$] 2147 *m/z* and 2165 *m/z*) (**c**) were detected for reduced PDI and auto-oxidized PDI displaying similar auto-oxidation patterns.

Redox-Induced Changes of b′ Domain Cysteines

The functional significance of the two cysteine residues within the *b′* domain of the human PDI has not been completely elucidated. Point-mutation studies suggest that these residues may not play any role in PDI catalytic activity or substrate interaction [19, 36–38]. We observed that following auto-oxidation, no change in the redox state of Cys-326 was detected ([MH$^+$] 1178 *m/z* and [MH$^+$] 1187 *m/z*) and, therefore, serves as an internal control for the reduced and auto-oxidized samples (Figure 6).

Interestingly, auto-oxidation did induce changes in the redox state of the other *b′* domain cysteine residue, Cys-295. Two differential cleavage peptides containing Cys-295 ([MH$^+$] 1470 *m/z* and [MH$^+$] 1479 *m/z*; [MH$^+$] 1728 *m/z* and [MH$^+$] 1737 *m/z*) demonstrated a dramatic loss of ICAT reactivity under auto-oxidized conditions (Figure 6). This result suggests, that in addition to changes within the *a* domain active site of human PDI, Cys-295 within the *b′* domain is also sensitive to redox regulation. This is interesting since a study involving chemical modification of an isolated *b′* domain indicated that neither of these cysteine residues are likely to exchange between dithiol and disulfide states upon

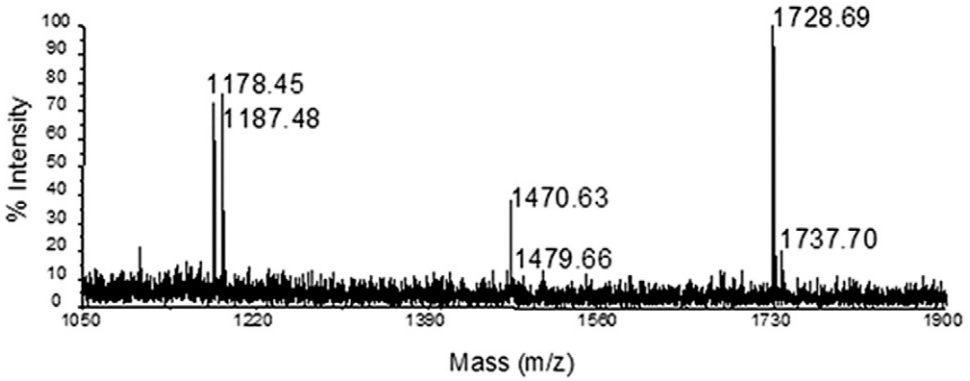

Figure 6. Redox regulation of Cys-295 within the *b′* domain. MALDI-TOF analysis of peptides containing *b′* domain Cys residues labeled with light and heavy ICAT. Similar levels of peptides containing Cys-326 from reduced (light ICAT) and auto-oxidized (heavy ICAT) samples were detected at [MH^+] 1178 *m/z* and [MH^+] 1187 *m/z* respectively. The Cys-295 containing peptides from two mis-cleavage products ([MH^+] 1470 *m/z* and [MH^+] 1728 *m/z* for light ICAT) show a 5-fold decrease in ICAT-labeling upon auto-oxidation ([MH^+] 1479 *m/z* and [MH^+] 1737 *m/z*).

modulation of redox potential [37]. In contrast, based on the crystal structure of yeast PDI, Cys-90 and Cys-97 were elucidated to form a disulfide bond [20]. These two nonactive site cysteines are believed to destabilize the oxidated state of the *a* domain active site cysteines [39]. Our results using full length PDI implicates Cys-295 may play a similar role as an additional redox sensitive site, potentially capable of modulating PDI activities.

Conclusion

This study reports detection and identification of redox induced changes on individual cysteine residues of recombinant human PDI in response to auto-oxidation conditions using ICAT methodology combined with mass spectrometry. The ICAT data presented here agree with the predicted susceptibility to oxidation of the active site vicinal thiols within the *a* domain, in that both of these cysteine residues were reactive towards ICAT-reagent in the fully reduced enzyme. However, the ICAT-signal of these thiols decreased by 5-fold upon auto-oxidation. Other previous studies have implicated that the *a′* domain is the higher oxidized active site [5, 21]. As predicted, our results are consistent with these studies and therefore demonstrates that ICAT technology is a reliable probe for the redox state of the *a* domain. However, specific conditions may exist that transform the *a′* domain to its reduced form. Under these specific conditions, this ICAT procedure should be capable of detecting and quantitating this transformation.

Since PDI activity is redox dependent and dynamically regulated; this approach will be useful to correlate what conditions favor the specific redox states of PDI. Studies are currently directed at applying this approach to monitor and quantify the redox alterations of different cellular pools of PDI in response to various environmental stimuli.

Acknowledgments

The authors thank John Hudson for critical reading of the manuscript. This project has been funded by a Grant-in-Aid from the Canadian Diabetes Association to B.M. and P.O.V. and a postgraduate scholarship by the Natural Sciences and Engineering Research Council (NSERC) to A.K.

References

1. Gilbert, H. F. Protein Disulfide Isomerase and Assisted Protein Folding. *J. Biol. Chem.* **1997,** *272,* 29399–29402.
2. Ellgaard, L.; Ruddock, L. W. The Human Protein Disulphide Isomerase Family: Substrate Interactions and Functional Properties. *EMBO Rep.* **2005,** *6,* 28–32.
3. Tsai, B.; Rodighiero, C.; Lencer, W. I.; Rapoport, T. A. Protein Disulfide Isomerase Acts as a Redox-Dependent Chaperone to Unfold Cholera Toxin. *Cell* **2001,** *104,* 937–948.
4. Janiszewski, M.; Lopes, L. R.; Carmo, A. O.; Pedro, M. A.; Brandes, R. P.; Santos, C. X.; Laurindo, F. R. Regulation of NAD(P)H Oxidase by Associated Protein Disulfide Isomerase in Vascular Smooth Muscle Cells. *J. Biol. Chem.* **2005,** *280,* 40813–40819.
5. Sliskovic, I.; Raturi, A.; Mutus, B. Characterization of the S-Denitrosation Activity of Protein Disulfide Isomerase. *J. Biol. Chem.* **2005,** *280,* 8733–8741.
6. Munro, S.; Pelham, H. R. A C-Terminal Signal Prevents Secretion of Luminal ER Proteins. *Cell* **1987,** *48,* 899–907.
7. Shin, B. K.; Wang, H.; Yim, A. M.; Le Naour, F.; Brichory, F.; Jang, J. H.; Zhao, R.; Puravs, E.; Tra, J.; Michael, C. W.; Misek, D. E.; Hanash, S. M. Global Profiling of the Cell Surface Proteome of Cancer Cells Uncovers an Abundance of Proteins with Chaperone Function. *J. Biol. Chem.* **2003,** *278,* 7607–7616.
8. Turano, C.; Coppari, S.; Altieri, F.; Ferraro, A. Proteins of the PDI Family: Unpredicted Non-ER Locations and Functions. *J. Cell. Physiol.* **2002,** *193,* 154–163.
9. Jiang, X. M.; Fitzgerald, M.; Grant, C. M.; Hogg, P. J. Redox Control of Exofacial Protein Thiols/Disulfides by Protein Disulfide Isomerase. *J. Biol. Chem.* **1999,** *274,* 2416–2423.
10. Pihlajaniemi, T.; Helaakoski, T.; Tasanen, K.; Myllyla, R.; Huhtala, M. L.; Koivu, J.; Kivirikko, K. I. Molecular Cloning of the β-Subunit of Human Prolyl 4-Hydroxylase. This Subunit and Protein Disulphide Isomerase are Products of the Same Gene. *EMBO J.* **1987,** *6,* 643–649.
11. Koivu, J.; Myllyla, R.; Helaakoski, T.; Pihlajaniemi, T.; Tasanen, K.; Kivirikko, K. I. A Single Polypeptide Acts Both as the β Subunit of Prolyl 4-Hydroxylase and as a Protein Disulfide-Isomerase. *J. Biol. Chem.* **1987,** *262,* 6447–6449.
12. Wetterau, J. R.; Combs, K. A.; Spinner, S. N.; Joiner, B. J. Protein Disulfide Isomerase is a Component of the Microsomal Triglyceride Transfer Protein Complex. *J. Biol. Chem.* **1990,** *265,* 9801–9807.
13. Lamberg, A.; Jauhiainen, M.; Metso, J.; Ehnholm, C.; Shoulders, C.; Scott, J.; Pihlajaniemi, T.; Kivirikko, K. I. The Role of Protein Disulphide Isomerase in the Microsomal Triacylglycerol Transfer Protein Does Not Reside in its Isomerase Activity. *Biochem. J.* **1996,** *315*(Pt 2), 533–536.
14. Edman, J. C.; Ellis, L.; Blacher, R. W.; Roth, R. A.; Rutter, W. J. Sequence of protein Disulphide Isomerase and Implications of Its Relationship to Thioredoxin. *Nature* **1985,** *317,* 267–270.
15. Koivunen, P.; Pirneskoski, A.; Karvonen, P.; Ljung, J.; Helaakoski, T.; Notbohm, H.; Kivirikko, K. I. The Acidic C-Terminal Domain of Protein

Disulfide Isomerase is Not Critical for the Enzyme Subunit Function or for the Chaperone or Disulfide Isomerase Activities of the Polypeptide. *EMBO J.* **1999,** *18,* 65–74.
16. Darby, N. J.; Kemmink, J.; Creighton, T. E. Identifying and Characterizing a Structural Domain of Protein Disulfide Isomerase. *Biochemistry* **1996,** *35,* 10517–10528.
17. Freedman, R. B.; Hirst, T. R.; Tuite, M. F. Protein Disulphide Isomerase: Building Bridges in Protein Folding. *Trends Biochem. Sci.* **1994,** *19,* 331–336.
18. Lundstrom, J.; Holmgren, A. Protein Disulfide-Isomerase is a Substrate for Thioredoxin Reductase and Has Thioredoxin-Like Activity. *J. Biol. Chem.* **1990,** *265,* 9114–9120.
19. Darby, N. J.; Penka, E.; Vincentelli, R. The Multi-Domain Structure of Protein Disulfide Isomerase is Essential for High Catalytic Efficiency. *J. Mol. Biol.* **1998,** *276,* 239–247.
20. Tian, G.; Xiang, S.; Noiva, R.; Lennarz, W. J.; Schindelin H. The Crystal Structure of Yeast Protein Disulfide Isomerase Suggests Cooperativity Between Its Active Sites. *Cell* **2006,** *124,* 61–73.
21. Lyles, M. M.; Gilbert, H. F. Mutations in the Thioredoxin Sites of Protein Disulfide Isomerase Reveal Functional Nonequivalence of the N- and C-Terminal Domains. *J. Biol. Chem.* **1994,** *269,* 30946–30952.
22. Kemmink, J.; Darby, N. J.; Dijkstra, K.; Nilges, M.; Creighton, T. E. Structure Determination of the N-Terminal Thioredoxin-Like Domain of Protein Disulfide Isomerase Using Multidimensional Heteronuclear 13C/15N NMR Spectroscopy. *Biochemistry* **1996,** *35,* 7684–7691.
23. Xiao, R.; Lundstrom-Ljung, J.; Holmgren, A.; Gilbert, H. F. Catalysis of Thiol/Disulfide Exchange. Glutaredoxin 1 and Protein-Disulfide Isomerase Use Different Mechanisms to Enhance Oxidase and Reductase Activities. *J. Biol. Chem.* **2005,** *280,* 21099–21106.
24. Burgess, J. K.; Hotchkiss, K. A.; Suter, C.; Dudman, N. P.; Szollosi, J.; Chesterman, C. N.; Chong, B. H.; Hogg, P. J. Physical Proximity and Functional Association of Glycoprotein 1b-α and Protein-Disulfide Isomerase on the Platelet Plasma Membrane. *J. Biol. Chem.* **2000,** *275,* 9758–9766.
25. Wright, S. K.; Viola, R. E. Evaluation of Methods for the Quantitation of Cysteines in Proteins. *Anal. Biochem.* **1998,** *265,* 8–14.
26. Gygi, S. P.; Rist, B.; Gerber, S. A.; Turecek, F.; Gelb, M. H.; Aebersold, R. Quantitative Analysis of Complex Protein Mixtures Using Isotope-Coded Affinity Tags. *Nat. Biotechnol.* **1999,** *17,* 994–999.
27. Hansen, K. C.; Schmitt-Ulms, G.; Chalkley, R. J.; Hirsch, J.; Baldwin, M. A.; Burlingame, A. L. Mass Spectrometric Analysis of Protein Mixtures at Low Levels Using Cleavable 13C-Isotope-Coded Affinity Tag and Multidimensional Chromatography. *Mol. Cell. Proteom.* **2003,** *2,* 299–314.
28. Bradford, M. M. A Rapid and Sensitive Method for the Quantitation of Microgram Quantities of Protein Utilizing the Principle of Protein-Dye Binding. *Anal. Biochem.* **1976,** *72,* 248–254.
29. Yen, T. Y.; Yan, H.; Macher, B. A. Characterizing Closely Spaced, Complex Disulfide Bond Patterns in Peptides and Proteins by Liquid Chromatography/Electrospray Ionization Tandem Mass Spectrometry. *J. Mass Spectrom.* **2002,** *37,* 15–30.
30. Kaetzel, R. S.; Stapels, M. D.; Barofsky, D. F.; Reed, D. J. Alkylation of Protein Disulfide Isomerase by the Episulfonium Ion Derived from the Glutathione Conjugate of 1,2-Dichloroethane and Mass Spectrometric Characterization of the Adducts. *Arch. Biochem. Biophys.* **2004,** *423,* 136–147.
31. Carbone, D. L.; Doorn, J. A.; Kiebler, Z.; Petersen, D. R. Cysteine Modification by Lipid Peroxidation Products Inhibits Protein Disulfide Isomerase. *Chem. Res. Toxicol.* **2005,** *18,* 1324–1331.
32. Thiede, B.; Lamer, S.; Mattow, J.; Siejak, F.; Dimmler, C.; Rudel, T.; Jungblut, P. R. Analysis of Missed Cleavage Sites, Tryptophan Oxidation, and N-Terminal Pyroglutamylation After In-Gel Tryptic Digestion. *Rapid Commun. Mass Spectrom.* **2000,** *14,* 496–502.
33. Taylor, S. W.; Fahy, E.; Murray, J.; Capaldi, R. A.; Ghosh, S. S. Oxidative Post-Translational Modification of Tryptophan Residues in Cardiac Mitochondrial Proteins. *J. Biol. Chem.* **2003,** *278,* 19587–19590.
34. Karty, J. A.; Ireland, M. M.; Brun, Y. V.; Reilly, J. P. Artifacts and Unassigned Masses Encountered in Peptide Mass Mapping. *J. Chromatogr. B Analyt. Technol. Biomed. Life Sci.* **2002,** *782,* 363–383.
35. Finley, E. L.; Dillon, J.; Crouch, R. K.; Schey, K. L. Identification of Tryptophan Oxidation Products in Bovine α-Crystallin. *Protein Sci.* **1998,** *7,* 2391–2397.
36. Schwaller, M.; Wilkinson, B.; Gilbert, H. F. Reduction-Reoxidation Cycles Contribute to Catalysis of Disulfide Isomerization by Protein-Disulfide Isomerase. *J. Biol. Chem.* **2003,** *278,* 7154–7159.
37. Pirneskoski, A.; Klappa, P.; Lobell, M.; Williamson, R. A.; Byrne, L.; Alanen, H. I.; Salo, K. E.; Kivirikko, K. I.; Freedman, R. B.; Ruddock, L. W. Molecular Characterization of the Principal Substrate Binding Site of the Ubiquitous Folding Catalyst Protein Disulfide Isomerase. *J. Biol. Chem.* **2004,** *279,* 10374–10381.
38. Klappa, P.; Ruddock, L. W.; Darby, N. J.; Freedman, R. B. The b′ Domain Provides the Principal Peptide-Binding Site of Protein Disulfide Isomerase but All Domains Contribute to Binding of Misfolded Proteins. *EMBO J.* **1998,** *17,* 927–935.
39. Wilkinson, B.; Xiao, R.; Gilbert, H. F. A Structural Disulfide of Yeast Protein-Disulfide Isomerase Destabilizes the Active Site Disulfide of the N-Terminal Thioredoxin Domain. *J. Biol. Chem.* **2005,** *280,* 11483–11487.